

Nanoscale

Accepted Manuscript



This is an *Accepted Manuscript*, which has been through the Royal Society of Chemistry peer review process and has been accepted for publication.

Accepted Manuscripts are published online shortly after acceptance, before technical editing, formatting and proof reading. Using this free service, authors can make their results available to the community, in citable form, before we publish the edited article. We will replace this *Accepted Manuscript* with the edited and formatted *Advance Article* as soon as it is available.

You can find more information about *Accepted Manuscripts* in the [Information for Authors](#).

Please note that technical editing may introduce minor changes to the text and/or graphics, which may alter content. The journal's standard [Terms & Conditions](#) and the [Ethical guidelines](#) still apply. In no event shall the Royal Society of Chemistry be held responsible for any errors or omissions in this *Accepted Manuscript* or any consequences arising from the use of any information it contains.

ARTICLE

Melt-Grafting for the Synthesis of Core-Shell Nanoparticles with Ultra-High Dispersant Density

Cite this: DOI: 10.1039/x0xx00000x

Ronald Zirbs,^a Andrea Lassenberger,^a Iris Vonderhaid,^a Steffen Kurzhals,^a Erik Reimhult^{a*}

Received 00th January 2012,
Accepted 00th January 2012

DOI: 10.1039/x0xx00000x

www.rsc.org/

Superparamagnetic iron oxide nanoparticles (NPs) are used in a rapidly expanding number of applications in e.g. the biomedical field, for which brushes of biocompatible polymers such as poly(ethylene glycol) (PEG) have to be densely grafted to the core. Grafting of such shells to monodisperse iron oxide NPs has remained a challenge mainly due to the conflicting requirements to replace the ligand shell of as-synthesized NPs with irreversibly bound PEG dispersants. We introduce a general two-step method to graft PEG dispersants from a melt to iron oxide NPs first functionalized with nitrodopamine (NDA). This method yields uniquely dense (~ 3 chains/nm²) spherical PEG-brushes compared to existing methods, and remarkably colloidally stable NPs also under challenging conditions.

ARTICLE

Introduction

Superparamagnetic iron oxide nanoparticles (NPs), with core diameters of 3-15 nm, are used in a rapidly expanding number of applications in the biomedical field; the most common include cell labeling,^{1, 2} hyperthermia,^{3, 4} drug delivery,⁵ and as contrast agents for magnetic resonance imaging.⁶⁻⁸ Iron oxide cores are coated with polymers, lipids or other dispersants to enable dispersion of NPs in aqueous solutions containing biomolecules. Rapid aggregation and precipitation occur without a sterically stabilizing shell. The most common methods to stabilize iron oxide NPs for biomedical applications have been to enwrap them in a weakly adsorbed shell of high molecular weight polymer (often dextran) or to coat them by self-assembling amphiphiles such as block copolymers or lipids. However, weakly adsorbed shells lead to low polymer densities on the particle surface and a lowered colloidal stability.⁹ Chemically grafted polymer shells provide a more stable option and has therefore received increasing attention and emphasis in recent years.¹⁰

With recent improvements in the synthesis of NPs,¹¹ there has also been a trend towards more well-defined, core-shell NP architectures.¹² Spherical iron oxide NPs can now be synthesized with monodisperse size and physical properties;¹³ these NPs require stabilization with a shell of linear, end-grafted polymer dispersants of sufficient thickness and grafting density to ensure that the particles remain individually dispersed and with uniform physicochemical properties during application. A defined core-shell architecture enables the prediction of all colloidal properties and serves as a platform for defining biological interactions through the attachment of organic ligands. The main advantage of grafting dispersants to the core is that the hydrodynamic size of NPs, stability of the shell and presentation of ligands can be precisely controlled in contrast to for NPs with dispersant shells consisting of physisorbed, high molecular weight dispersants;¹² this critically determines NP performance in a biological fluid.^{14, 15}

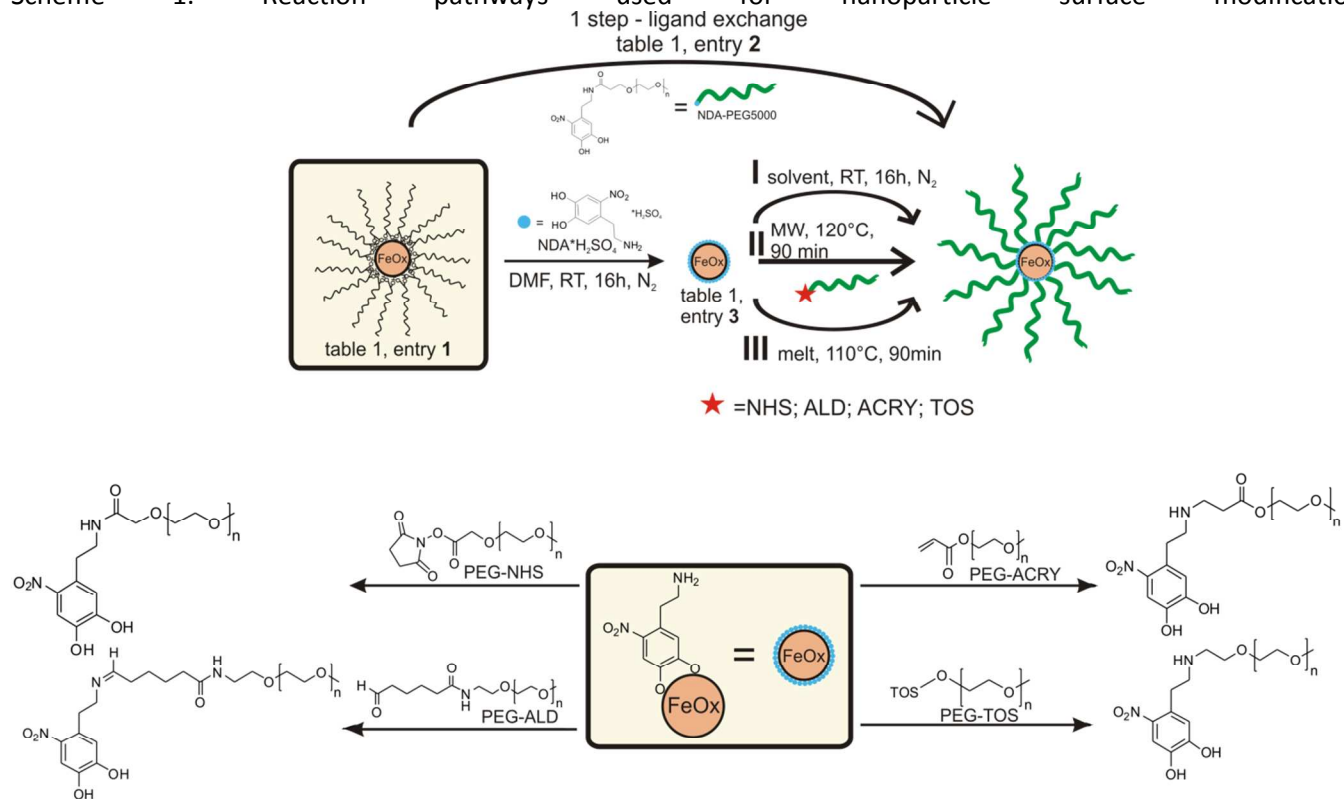
The maximum achieved grafting densities on planar substrates of PEG(5kDa) are in the range of 0.4 chains/nm².¹⁶ NP

curvature facilitates polymer grafting by increasing the specific volume available per dispersant and grafting densities up to 2.5 chains/nm² have been claimed on iron oxide NPs.^{10, 17} An irreversibly grafted shell of >2chains/nm² of PEG(5kDa) on polydisperse and irregularly shaped single NPs was also shown to be required for colloidal stability under application conditions such as high salt concentration, high dilution and elevated temperature. However, only grafting densities of ~0.5chains/nm² have been reported on spherical Fe₃O₄ NPs, for which the grafting requires replacement of an already adsorbed ligand.¹⁸

We have previously demonstrated that colloidal stability can be achieved by direct grafting of PEG using nitrocatechol anchors to form an irreversible bond to bare Fe₃O₄ NPs.^{10, 19} Synthesis of truly monodisperse (SD<5%) Fe₃O₄ core-shell NPs makes use of e.g. oleic acid (OA) ligands to control crystal growth.²⁰ The as-synthesized NP core has a dense shell of OA that has to be replaced by the stabilizing dispersant. Similarly monodisperse, but not as spherical, NPs have been synthesized using oleylamine instead of oleic acid. Oleylamine has the advantage that it can more easily be removed from the NP surface compared to oleic acid, due to its weaker binding. Ligand replacement of oleylamine by nitroDOPA-PEG therefore has been demonstrated.¹⁸ However, these NPs possessed ~5 times lower PEG grafting density (~0.5chains/nm²) and thereby significantly lower colloidal stability than NPs that were synthesized without capping agents and grafted with nitroDOPA-PEG. The low grafting efficiency is the result of simultaneously trying to fulfill several mutually contradicting conditions during the ligand replacement reaction: (1) to dissolve the capping agent (oleic acid), (2) to solubilize the dispersant, (3) to keep the dispersant at low coil size, quantitatively described by e.g. R_G , which determines the grafting footprint, and (4) to provide the right conditions (protonation) of the anchor group to irreversibly bind to the core.

ARTICLE

Scheme 1. Reaction pathways used for nanoparticle surface modification.



Schematic representation of direct ligand exchange and the two-step grafting-to method for the synthesis of core-shell NPs. **Bottom:** Schematic representation of the different grafting-to reactions. The NHS-activated coupling leads to a stable amide-bond, acrylates undergo a Michael-addition to form secondary amines, aldehyde reacts under condensation forming an imine and PEG-tosylate with nucleophilic-substitution to form a secondary amine.

We have investigated the consequences of these limits on PEG grafting to iron oxide NPs synthesized by the method of Park et al.,^{11, 13, 18, 21, 22} by this synthesis method monodisperse, spherical NPs capped with OA are obtained. The goal was to obtain a dense shell of PEG(5kDa) irreversibly bound to the Fe₃O₄ core through nitrodopamine (NDA). The shell density should exceed the ~ 2 PEG(5kDa)/nm² that seems to be the threshold for high colloidal and temperature stability.^{10, 12} Pre-synthesized PEG dispersant thus has to completely replace the OA on the monodisperse iron oxide NP surface in a grafting-to approach.

We choose to evaluate three different reaction environments for grafting-to: a) reaction in solution (**I**); b) microwave (MW) assisted reaction in poor solvent like methanol (**II**) and c) reaction in polymer melt (**III**). These grafting methods were chosen to compare the proposed novel and improved grafting methods (**II**, **III**) to the method representative of the state-of-the-art (**I**, direct ligand replacement of NDA-PEG in solution).

The first part of the philosophy behind both the MW-assisted and polymer-melt grafting approaches is to minimize the PEG coil size during the grafting reaction. The effective coil size during grafting will determine the maximum packing of polymer on the particle surface and thereby the average distance between grafting sites. The absolute highest achievable grafting density will additionally be determined by the deformability and intercalation of the polymer coils at the NP surface; it is likely closer than the distance given by the steric size of the coils. Without being able to specify the closest possible spacing between grafting sites in terms of a specific measure of the polymer coil size, we propose that minimizing a suitable measure of the size of the coil, such as the radius of gyration, R_g , will on average lead to increased grafting density if chain flexibility and dynamics are maintained. Retained chain dynamics is important, because grafting of the polymer will only occur if sufficient reactivity of the polymer end-group at the coil surface is preserved. A compact coil under poor solvent conditions is known to lead to reduced surface accessibility of

reactive end-groups and to lead to lower effective reactivity. However, if dense grafting under collapsed coil conditions is achieved, swelling of the densely grafted polymer in the application environment will result in a thicker and denser shell due to the scaling of spherical brush thickness with grafting density.

The second part of our philosophy is to separate the grafting-to into steps of i) removing the oleic acid from the surface and ii) the reaction of the end-functionalized PEG to the surface, which can be separately optimized. To achieve this, we first replace the oleic acid in DMF with the strongly binding NDA.¹⁰ Nitrodopamine can due to its small size, high solubility and affinity for Fe₃O₄ in DMF much more easily perform the ligand replacement than a bulky end-functionalized PEG-chain; it also, after successful replacement, provides a high density of amine groups on the NP surface to which a greater variety of chemical reactions can be performed than to the Fe₃O₄ surface. Thus, grafting-to through ligand replacement was compared to first priming the NP surface with NDA and then reacting end-modified PEG-chains to the NDA-modified surface in a low solvation, i.e. low R_G or coil size, conformation. (Scheme 1).

Experimental

Reagents and materials

All chemicals were purchased from Sigma-Aldrich and were used without further purification.

PEG-ALD: O-[2-(6-Oxocaproylamino)ethyl]-O-methylpolyethyleneglycol 5000;

PEG-ACRY: Poly(ethylene glycol) methyl ether acrylate;

PEG-TOS: Poly(ethylene glycol) methyl ether tosylate;

PEG-NHS: Methoxypolyethylene glycol 5,000 acetic acid N-succinimidyl ester; purchased from JenKem-USA (Mn~5000; PDI=1.1; functionality of the end group >95%)

Carl Roth dialyzing membranes (regenerated cellulose) with a cut-off size of 5000 Da were used to purify the nitrodopamine modified NPs.

Synthesis of monodisperse Fe₃O₄ nanoparticles

An optimized thermal decomposition method analogous to Park et al. was used to synthesize monodisperse, monocrystalline Fe₃O₄ NPs.^{11, 13, 18, 21, 22} To prepare monodisperse iron nanoparticles, Fe(CO)₅ (1 mL; 1.49 g; 7.4 mmol) was added to a mixture containing 25 mL of dioctylether and 3 mL oleic acid (10 mmol) at 100°C. The resulting solution is heated to 290°C with a heating rate of 10 K/min (reflux) and kept at that temperature for 1 hour. To gain full reproducibility and control over the temperature during the NP synthesis a thermo controller LTR 3500/S from Juchheim-Solingen was used. During this time the color changes from the initial orange to dark black. The crude product was poured into 175 mL nitrogen-bubbled acetone after cooling the mixture to room temperature. After centrifugation (5000 rpm, 10 min, 20°C), the black product was redispersed in a small amount of toluene (~1 mL) and reprecipitated in acetone (190 mL). This

centrifugation-redispersion-precipitation step was repeated 3 times. The resulting oleic-acid-protected iron oxide NPs were used immediately for further reactions. The size of the particles could be controlled by the ratio of the iron pentacarbonyl and the oleic acid. Particles with a diameter of 3.8±0.3 to 6.4±0.4 nm have been used for the presented work.

Ligand-exchange with nitrodopamine-PEG5000-OMe (one-step-method)

The oleic-acid-covered NPs (25 mg) were dispersed in 20 mL DMF (headspace grade 99.99%, anhydrous) and nitrodopamine-PEG(5000) (500 mg; 0.1 mmol) (see SI for synthesis) was added. This solution was purged with nitrogen for 5 minutes, put in an ultrasonic bath for 60 minutes, allowed to stand at room temperature for 15 hours, ultrasonicated again for 60 minutes and precipitated in cold acetone (180 mL). After centrifugation and 5 washing steps (redispersion in methanol – centrifugation with 5000 rpm, 10 minutes, 20°C) the obtained core-shell iron oxide NPs (FeOx-PEG) were characterized using TEM, TGA and DLS.

Ligand-exchange of oleic acid to nitrodopamine

The oleic acid-covered NPs (~3 g) were dispersed in 20 mL DMF (headspace grade 99.99%, anhydrous) and nitrodopamine hydrogensulfate (450 mg; 1.5 mmol) was added. This solution was purged with nitrogen for 2 minutes, put in an ultrasonic bath for 60 minutes, allowed to stand at room temperature for 15 hours, ultrasonicated again for 60 minutes and precipitated in pure acetone (180 mL, cold). After centrifugation and 5 washing steps (redispersion in methanol – centrifugation at 5000 rpm, 10 minutes, 20°C) the obtained nitrodopamine modified iron oxide NPs were used directly for grafting with PEG.

Synthesis of PEGylated core-shell nanoparticles using grafting-to reaction in solution (scheme 1; method I)

The as-synthesized NDA-modified NPs (50 mg) were dissolved in dry DMF (5 mL, headspace grade 99.99%, anhydrous), the respective PEG-derivate (500 mg, 0.1 mmol, NHS, TOS, ALD) was added and the mixture was stirred at room temperature for 16 hours. After pouring the reaction mixture into 195 mL cold acetone and centrifugation (5000 rpm, 10 minutes, 4°C) the precipitate was dissolved in water (2 mL), filtered through a 0.45 µm syringe filter to remove aggregates and purified as described below.

Synthesis of PEGylated core-shell nanoparticles using microwave assisted reactions (scheme 1; method II)

The as-synthesized NDA-modified NPs (50 mg) were dissolved in dry methanol (3 mL). The respective PEG-derivate (500 mg; ~0.1 mmol; NHS; ACRY; TOS; ALD) was added and this mixture was heated in a CEM lab microwave to 120°C for 90 minutes. After cooling to room temperature the reaction mixture was poured into 190 mL cold acetone and centrifuged for 10 minutes at 5000 rpm (4°C). The precipitate was

dissolved in water (2 mL), filtered through a 0.45 μm syringe filter to remove aggregates and purified as described below.

Synthesis of PEGylated core-shell nanoparticles using polymer melts (scheme 1; method III)

The freshly synthesized NDA-modified NPs (~50 mg) were mixed with the dry PEG-derivate (TOS, NHS, ALD, ARCY) (500 mg; 0.1 mmol), purged with nitrogen and slowly heated to 110°C. After the material was completely molten a nitrogen-flow (needle) was used to mix the melt continuously. The reaction was kept at this temperature for 90 minutes. After cooling to room temperature, the black solid was dissolved in water (2 mL) (ultrasonic bath for 1 hour), filtered through a 0.45 μm syringe filter (RC) to remove aggregates and purified as described below.

Purification of PEG-grafted iron oxide core-shell nanoparticles

The dark PEG-grafted iron oxide NP solution in water was applied onto a 25 cm long (3 cm diameter) column filled with Sephadex G75 (milli-Q water, separation range $1 \times 10^3 - 5 \times 10^4$ g/mol for dextrans). Pure Milli-Q water was used for the purification. Fractions of 5 mL were collected, after filtering the single fractions through 0.45 μm syringe-filters and freeze dried. The products were characterized using TEM, TGA and DLS.

Characterization of the core-shell nanoparticles using TEM

A small amount of product was dissolved in water (nitrodopamine and PEG-modified particles) or toluene (oleic acid modified NPs) and dropped onto the TEM-grid (3.05 mm HR-TEM-grid, copper 300 mesh, carbon film, Gröpl Austria). All pictures were taken using a FEI TECNAI G2 at 200 kV.

Characterization of the core-shell nanoparticles using TGA

1-10 mg of sample was weighed into 70 μL AlOx-cups and measured on a Mettler-Toledo TGA/DSC 1. The samples were measured in a constant flow of synthetic air (80 mL/min plus 20 mL nitrogen stream as protection gas for the balance) with a heating rate of 10 K/min. Analysis was performed using the Mettler-Toledo software (simple step-function from 200-550°C).

Characterization of the core-shell nanoparticles using ATR-FTIR

Mid-IR powder spectra of the lyophilized samples were collected using a Bruker Tensor 37 FTIR spectrometer with a Bruker Platinum Diamond single reflection ATR equipment at a resolution of 4 cm^{-1} by averaging 32 scans.

Characterization of core-shell nanoparticle hydrodynamic size and tests of colloidal stability of nanoparticles in ethanol and PBS

The different iron oxide NPs (one-step ligand exchange particles: Table 1, 2 and ALD-melt grafting-to particles: Table 1, 15) were dissolved in water (0.5 mg/mL) and placed into a Malvern Zetasizer Dynamic Light Scattering (DLS) instrument. After equilibrating at 25°C the hydrodynamic size distribution

was measured every hour using the built in fitting based on the CONTIN algorithm.

After 2 hours of recorded size stability in water, 10 weight% of ethanol was added to the cuvette, which was shaken intensely for 3 seconds, and placed back into the instrument. Measurements of the hydrodynamic size were performed for 8 more hours.

The stability of the NPs in phosphate buffered saline (PBS) buffer was tested by dissolving 0.5 mg of the ALD-melt grafted NPs (table 1, 15) and the one-step ligand exchange NPs (Table 1, 2) in water and PBS. The cuvettes were placed in the DLS instrument, heated to 85°C and data was collected every hour for 15 hours.

Test of colloidal stability of NPs upon heat treatment in serum

1 mL of fetal calf serum (FCS) was placed into DLS cuvettes. 0.5 mg of either the ALD-melt NPs (Table 1, 15) or the one-step ligand exchange NPs (Table 1, 2) was added to the FCS and the cuvette was gently shaken until the solution was homogeneous. The hydrodynamic size was thereafter measured every hour for 10 hours by DLS.

Results and discussion

Monodisperse core-shell nanoparticle synthesis

The NPs were synthesized by an optimized heat-up process following Park et al.,^{11, 13, 18, 21-23} leading to monocrystalline Fe_3O_4 NPs with well-defined size (diameter adjustable between 3.5-9 nm; SD = 5%), and high sphericity (Figure 1). Grafting experiments used NPs of two different sizes 3.8 ± 0.3 and 6.4 ± 0.4 nm; the first size corresponds to the smallest part of the range where spherical and magnetic NPs are obtained, and the second size is in the middle of the superparamagnetic size range. The core sizes were obtained by the use of the freeware Pebbles,²⁴ which analyses images with hundreds of NPs to produce size distributions for calculation of mean size and size standard deviation (see SI).

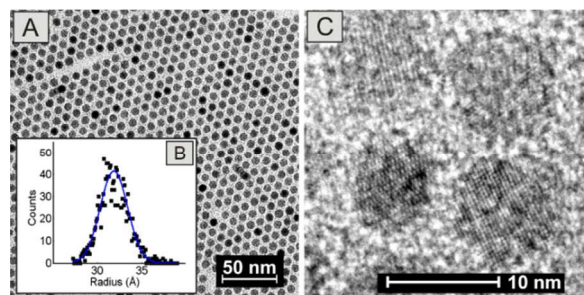


Figure 1. (A) Transmission electron microscopy image of 6.4 ± 0.4 nm Fe_3O_4 NPs. The particles show excellent monodispersity (SD<5%) (B) and are monocrystalline (C).

All grafting methods were performed as described in the Experimental section with an excess of free polymer. The mole amount of polymer added for the grafting reactions was double the total number of NDA binding sites calculated from the grafting density measured by TGA (Table 1, 3) and taking into

account the core size-dependent total surface area of the sample. The excess was added to ensure that the maximum possible grafting density could always be achieved.

Purification and characterization of core-shell iron oxide nanoparticles

A key step to characterize polymer-grafted core-shell NPs is the removal of residual dispersant from the sample. Previous works by us and others indicate that magnetic decantation, dialysis and centrifugation can lead to substantial residual dispersant, while size exclusion chromatography can separate free PEG from grafted particles.¹² Size exclusion chromatography by dextran column can also be used to evaluate the colloidal stability of iron oxide NPs since iron oxide has high affinity for dextran; insufficiently densely grafted particles bind to the dextran column. All samples were therefore purified using a 25cm long and 3cm broad Sephadex G75 column. This length was chosen as it generated distinguishable fractions for further analysis. Fractions were collected manually, separated every 5mL, filtered through a 0.45 μ m syringe filter and freeze dried to obtain the products. Each fraction of each sample could thus be analyzed to determine its polymer content, iron oxide core content, hydrodynamic radius and colloidal stability. A high percentage of the NPs can stick to the Sephadex material during the separation process; this lost fraction is considered to be composed of poorly grafted NPs; it will also contain aggregated parts of the raw product. As discussed below, the amount of material lost to column purification varied greatly with the preparation protocol, and could be used as a tool also to estimate the homogeneity of the product in terms of grafting density. We define the yield of a modification protocol as the amount of iron oxide NP found in the best product fraction relative to the original amount of iron oxide NP material added to the beginning of the synthesis. The amount was measured by the non-organic content determined by TGA.

Samples obtained by direct ligand exchange of OA for NDA-PEG bound completely to the column due to the obviously low grafting density that was achieved. These samples were instead purified using repeated centrifugation in methanol/acetone mixtures and using magnetic extraction; residual PEG could be present in the samples after this purification and lead to an overestimated grafting density.

Investigation of grafting density by different grafting methods

The success of the grafting methods can be compared on a set of dependent criteria such as grafting density, colloidal stability, cost and ease of synthesis. Grafting density was our primary concern as particle stability is derived from grafting density; it was determined by TGA for each method and fraction.

Table 1 shows the results obtained for the highest grafting density fraction for all protocols applied to 3.8nm cores. The first test was performed using direct ligand replacement of OA for NDA-PEG. Ligand replacement of OA for NDA-PEG requires solvents, e.g. DMF, that strike a compromise between sufficiently high solubility of both OA and PEG and a low R_G

(solvated coil size) of the PEG. The R_G of PEG in DMF is above its theoretical minimum, which limits the highest obtainable PEG grafting density (Table 1, 2). The achieved density of 0.5 ± 0.2 chains/nm² after excess PEG removal is lower than required for dextran column purification, It is also lower than what has been reported necessary to achieve NPs stable under high salt, protein or temperature conditions, although due to different purification and testing conditions the literature is not conclusive on the minimal required grafting density.^{6, 12}

Table 1. Overview of the calculated grafting densities of PEG(5kD) obtained by grafting-to reactions to 3.8nm iron oxide cores evaluated by TGA after Sephadex G75 column purification.

#	Reactant	Method	Grafting density [chains/nm ²]	Yield [%]
1	FeOx-oleic acid		17.4 \pm 5 ^[e]	
2	nitrodopamine-PEG5000	one step grafting-to solution (DMF)	0.5 \pm 0.2 ^{[d][f]}	
3	FeOx-nitrodopamine	two step grafting-to procedure		
4	PEG-NHS	solution ^[a]	3.8 \pm 1.2	
5	PEG-TOS	solution ^[a]	0.9 \pm 0.2	
6	PEG-ACRY	solution ^[a]	0.8 \pm 0.6 ^[d]	
7	PEG-ALD	solution ^[a]	0.8 \pm 0.3	
8	PEG-NHS	MW ^[b]	1.0 \pm 0.3	
9	PEG-TOS	MW ^[b]	1.6 \pm 0.8	<5
10	PEG-ACRY	MW ^[b]	1.3 \pm 1	7 \pm 3
11	PEG-ALD	MW ^[b]	^[d]	
12	PEG-NHS	melt ^[c]	^[d]	
13	PEG-TOS	melt ^[c]	1.1 \pm 0.5 ^[f]	<5
14	PEG-ACRY	melt ^[c]	2.2 \pm 0.4 ^[f]	8 \pm 5
15	PEG-ALD	melt ^[c]	3.1 \pm 0.9 ^[f]	16 \pm 5
16	PEG-ALD	melt ^[g]	3.1 \pm 0.6	35 \pm 15

[a] 50 mg iron oxide-nitrodopamine particles, 500 mg PEG-X, 3 mL DMF, 16 h at RT [b] 50 mg iron oxide-nitrodopamine particles, 500 mg PEG-X, 3 mL MeOH, 90 min at 120°C [c] 50 mg iron oxide-nitrodopamine particles, 500 mg PEG-X, N₂-stream, 90 min at 110 °C [d] sample purified by 3 precipitation steps in acetone, [e] large amount of free oleic acid present, [f] measured identical also for 6.4nm particles, [g] melt was conducted under vacuum (4-8 mbar) and rotated with 100 rpm on a rotary evaporator

For all other grafting methods, OA was first completely replaced by NDA. This reaction can be carried out in an ideal solvent for OA and NDA, e.g. DMF, and results in \sim 4 NDA/nm² determined by TGA (Table 1, 3).

Several methods to bind PEG with a reactive end-group to the free amines of NDA-modified iron oxide NPs can be envisioned. We tested: a) tosylate (TOS) reacting with primary amines under a SN₂ reaction; b) acrylate (ACRY) enabling Michael-addition; c) aldehyde (ALD) enabling condensation (Mannich-reaction); and d) NHS activated acid enabling formation of an amide.

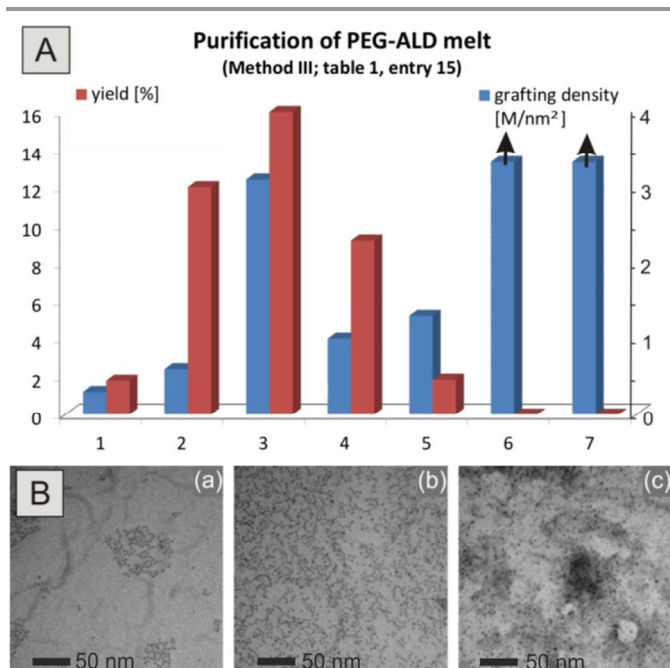


Figure 2. **A)** Results of column purification of a typical two-step synthesis (ALD-melt; Table 1, 15). Fractions were collected every 5 mL (x-axis). The yield after freeze-drying (red bars) calculated on the percentage of iron oxide cores in relation to the amount at the start of the synthesis and the apparent average grafting density (blue bars) calculated on the total organic content are shown for each fraction. Fraction 3 is the product fraction and Fraction 6 and Fraction 7 consist of almost pure PEG (bars truncated). **B):** TEM-pictures of main fractions of an ALD-melt (Table 1, entry 15). (a) Fraction 1 shows few aggregates with small particle-particle distances; (b) fraction 3 (main fraction) shows no aggregation and no free PEG, whereas in (c) (fraction 5) one can immediately identify huge areas of free (unbound) PEG.

Figure 2A shows the yield and the estimated grafting density of each sample fraction collected after the Sephadex column purification for NPs grafted by ALD-melt under bubbling with nitrogen (Table 1, 15). The yield is calculated as the percent of iron oxide cores found in each collected fraction in relation to the total amount of iron oxide cores at the start of the synthesis. The grafting density is calculated from the total organic content (TOC) fraction measured by TGA for each collected 5mL fraction. This apparent grafting density only corresponds to a real average grafting density for sample fractions containing iron oxide cores and no free PEG.

A high grafting density fraction (Fraction 3) with relatively high yield compared to other fractions was selected as the product. We emphasize that yields significantly lower than 100% after such demanding purification are acceptable given the high-end applications, and that the yield can be “increased” by enlarging the selection of the fraction in line with the demands of the application. The selected Fraction 3 with an average grafting density of 3.1 chains/nm² and average yield of up to 35% shows individual, well separated iron oxide cores inspected by TEM (Fig. 2B-b). Aggregated cores with <0.2 chains/nm² were collected before the main peak (Fr. 1-2), as evidenced by the sample TEM in Fig. 2B-a. Free PEG was collected in the final fraction(s), well separated from the product fraction. Fraction 5 already shows free PEG in the

background when investigated by TEM, with only few visible cores (Fig. 2B-c); for Fr. 6 and above essentially no particles can be imaged and only PEG is found in the sample. The much smaller and flexible PEG(5kDa) is trapped meandering for much longer time in the small-porous Sephadex G75 column, which makes size-exclusion chromatography a very efficient method for separation of densely grafted NPs from free polymer. Repeated column passes does not change the observed TOC measured by TGA, while large amounts of free polymer are removed during the first pass.

The highest average ligand density of product after column purification for each two-step grafting-to method is also given in Table 1, i.e. corresponding to Fraction 3 in Figure 2. The ligand density is calculated from the TOC measured by TGA for at least 3 repetitions of each synthetic protocol and selecting the best possible fraction in the same way as described for the ALD-melt sample. Table 1, 4-7 shows that almost all two-step coupling strategies in DMF improve the grafting density to ~1 chain/nm² compared to direct ligand replacement. This increase in average grafting density was sufficient for a fraction of spherical PEG-grafted NPs to pass column purification. The same reactions were also tested in a MW reactor (Table 1, 8-11). The MW heating of the NPs speeds up the grafting reactions and enables performing them in MeOH. MeOH reduces PEG solvation and thereby the coil size compared to DMF; this should increase the surface packing density and could therefore lead to higher grafting density. However, the MW-assisted reactions insignificantly improved the grafting density, which indicates that none of the reactions had increased efficiency for surface grafting under these conditions. The low yield and lack of major improvement in terms of grafting density could be due to a low surface availability of the reactive end-group under these solvent conditions. The highest average grafting density of the MW-assisted reactions was obtained for TOS-PEG (Table 1, 9), which provides the coupling reaction with the expected highest reactivity under these conditions, but the yield was still low.

A limitation that all of the above strategies have in common is that the footprint of the PEG-coil is not minimized during grafting. The reaction efficiency can be increased at the same time as the polymer footprint is minimized by choosing a reaction that performs at a temperature at which PEG(5kD) is in a pure melt and is fluid without added solvent. The pure melt has the advantage that due to the high temperature the chain mobility is still high, which could improve the accessibility of the reactive chain end-group and allow grafting at distances even closer than the steric coil size. Chain relaxation dynamics are expected to be well below sub-second. The grafting-to melt-reaction is performed for more than an hour, which leaves ample time for the chain to rearrange into possible binding configurations.

Grafting in a melt was first performed by slowly heating the NPs dispersed in pure PEG to 110°C. A flow of nitrogen was used for continuous mixing at constant temperature for 90 min. The best fractions using this method (Table 1, 12-15) far surpass the other methods in terms of grafting density. Grafting

densities of 2-3 chains/nm² were consistently achieved. This is ~25% below the ~4 NDA/nm² possible grafting sites and at least 2 times higher than for the other grafting methods. We emphasize again (Fig. 2A) that any free PEG is well separated from the NPs by column purification and that passes on the column did not change the measured grafting density. FTIR spectroscopy demonstrated that the OA had been fully replaced and the true NDA-PEG grafting density had been measured for the ALD-PEG product fraction, i.e. **Fr. 3** (Figure 3).

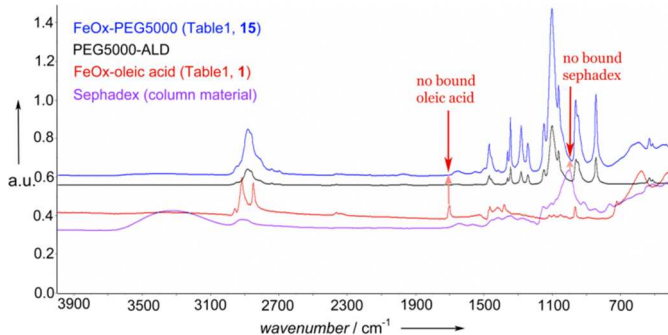


Figure 3: FTIR spectrum of the main product (ALD-melt, Fraction 3; table 1; entry 15) showing the absence of OA and dextran, but the presence of NDA-PEG.

The two-step melt graft-to method was also investigated on 6.4nm-core particles. The grafting densities were within the standard deviation equal and in fact near identical to those on 3.8nm cores for PEG-TOS and PEG-ALD, while no sample of PEG-ACRY was produced that could be purified by column. Also the obtained yields were similar.

It is clear that under equal conditions (same type of core synthesis, same anchor group and dispersant and same purification conditions) the melt graft method far outperforms previously employed or other here introduced methods to achieve high grafting density on monodisperse iron oxide NPs. Since we consistently compare the direct dispersant exchange, MW and melt two-step grafting approaches on the same cores and with the same methods, we can clearly state that the latter method is superior by at least a factor of 2. It outperforms direct ligand replacement, which did not yield stable monodisperse NPs, by a factor >4.

The existing literature does not provide any examples of PEG-grafting to similar monodisperse cores. A direct comparison to reports in the literature for other systems is difficult to perform in absolute terms due to the different purification, measurement and fitting methods that have been employed, in addition to that more polydisperse NPs lead to uncertainties in how to interpret the grafting densities that are described. However, the densities that we report for the melt-grafted NPs are higher than the highest reported for grafting also onto shape and size polydisperse bare iron oxide NPs of ~2.5 chains/nm², for which the purification protocol was similarly rigorous.¹⁰ An irregular core shape leads to underestimation of the true surface area and increases surface accessibility. This can together with that

ligand replacement was not required explain the high grafting density compared to our control with direct grafting of NDA-PEG to monodisperse NPs under the same conditions. To estimate the relative efficiency of the two methods, the direct comparison of the methods presented in this paper is the better guide.

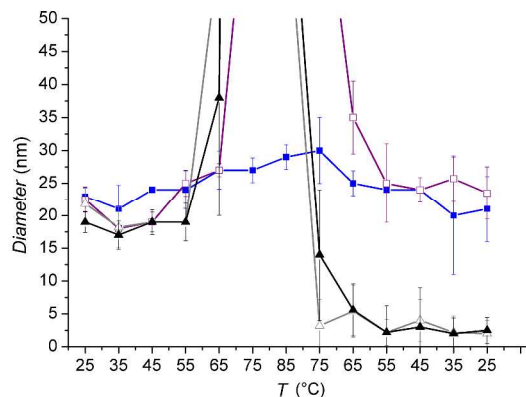


Figure 4: DLS of NP hydrodynamic diameter during *T*-cycling in water and PBS for NPs grafted with PEG by one-step ligand exchange (table 1, 2; black and grey lines with closed and open triangles respectively) and by the two-step ALD-melt method (table 1, 15; blue and purple curves with closed and open squares respectively). Average and standard deviations for at least 4 measurement series per type of sample are shown. In both aqueous environments only the ALD-melt grafted particles are colloiddally stable over the temperature cycle. The aggregation of the one-step ligand exchange particles leads first to increased average hydrodynamic size of the clusters, followed by precipitation and correlating loss of recorded size. The two-step, ALD-melt grafted particles show only reversible aggregation in PBS and no aggregation in water.

Optimization of the melt grafting method to improve the yield (scheme 1, method III)

Optimally, both grafting density and yield should be high for a successful NP surface modification protocol. Although the MW-assisted TOS-PEG (Table 1, 9) and ACRY-PEG melt reactions (table 1, 14) lead to high grafting densities (1.6 and 2.2 chains/nm²) the yields are low compared to the melt-grafted ALD-PEG (3.1 chains/nm²). In both cases the yield is <1/3 of that for ALD-PEG. The yields were very similar, but on average slightly lower for 6.4-nm-core particles. This could reflect that a good dispersion of NP cores in the polymer melt is more difficult to achieve for larger cores. More efficient bubbling using inert gas could potentially improve the mixing and thereby the yield.

Bubbling with inert gas also serves a second purpose, which is to remove water that is produced during the reaction. We therefore also attempted the synthesis under vacuum suction to more efficiently achieve continuous removal of water. Thus, the NDA-coated particles were dispersed in a small amount of dry THF (1mL/50mg particles) and added to the ALD-PEG, followed by slow drying in vacuum. Subsequently, the mixture was heated under continuous vacuum suction to conduct grafting under melt condition. Thereby, the yield of the ALD-melt could be improved from ~16% to ~35% (Table 1, 16). Although the yield was consistently higher with the improved procedure, the high variability in the yield suggests that further

optimization of the reactor vessel environment to improve NP dispersion and water removal can be made and thereby the yield could further be increased significantly.

Effect of dispersant grafting density on colloidal stability in aqueous suspension

That higher brush grafting density leads to higher colloidal stability under application of physiological conditions is a well-accepted hypothesis;¹² in biological fluids the colloidal stability of bare NPs is severely compromised due to high concentrations of ions and biomolecules such as proteins. The higher temperature than room temperature experienced in many applications of magnetic NPs has also been shown to lead to reduced colloidal stability of poorly grafted NPs or of NPs with reversibly anchored dispersants.^{10, 25} Temperature cycling can thus be used as an additional relevant stress test to compare the colloidal stability of differently synthesized NPs.¹²

Redispersion of strongly aggregated, dried NPs can be challenging, but the densely melt-grafted monodisperse NPs demonstrate remarkably easy redispersion. Dried powder dispersed instantly upon addition of the smallest amount of water; this indicates that the cores even in the dried state do not come in close proximity to each other. The supreme colloidal stability was further demonstrated by high stability in water over prolonged period of time (>1 year) and repeated filtering through 0.45- μm syringe filter without loss of material.

DLS showed that melt-grafted ALD-PEG NPs remained stable in size under temperature cycling in water (Fig. 4), which produced aggregation of NPs more sparsely grafted using one-step ligand exchange. ALD-PEG melt-grafted NPs showed reversible aggregation without precipitation upon T -cycling in PBS buffer (Fig. 4). PBS frequently leads to stronger aggregation of bare or weakly grafted iron oxide cores due to the strong interaction of phosphate ions and iron at the NP core surface. The one-step grafted NPs again demonstrated severe aggregation followed by precipitation during the same T -cycle in PBS. Experiments testing the resistance to precipitation in ethanol likewise showed that melt-grafted ALD-PEG NPs remained stably dispersed and could be filtered through 0.45 μm syringe filter, while other grafting methods led to precipitation (see SI).

Colloidal stability of NPs upon heat treatment in serum

Finally, the stability of NPs in the presence of serum was investigated. Stability at room temperature was observed over experimental time scales also for NPs with grafting densities <1 chain/nm². This can be the effect of NPs showing sufficient stability after adsorption of the albumin predominant in serum to not precipitate. BSA is commonly used as an easy and low-cost surface modification for biotechnological applications in *ex vivo* body fluids; however, it is not sufficient to stabilize NPs or other interfaces *in vivo*. It was not possible to efficiently separate NPs and proteins e.g. on a magnetic column, due to the high stability; this in itself demonstrates that the interaction with highly concentrated protein solutions does not lead to strong aggregation of the cores, but it could not be used to

differentiate between strongly and weakly stabilized NPs. The low effective density of the NPs (>80% of the mass is highly hydrated PEG shell) also foiled our attempts to use centrifugation to separate protein and NPs. Several different centrifugation and filtration separation methods were tested to analyse any potential protein content adhering to the NPs, but none were successful, i.e. a single dispersion always remained. A test was instead devised that used the denaturation and precipitation of serum at high temperature (75°C) to demonstrate the difference in protein interaction between NPs grafted by the two-step melt method and the one-step ligand replacement method. Denatured proteins adsorbing to an insufficiently protected NP surface at high T are likely to aggregate with other proteins and to precipitate the aggregates together with the NP out of solution. If the denatured proteins cannot directly adsorb to the NP surface a much smaller fraction of NPs would be trapped by such aggregates and precipitate.

Figure 5A shows the precipitation in the presence of serum protein. A majority fraction of NPs grafted by one-step ligand replacement precipitates with the protein when the protein denatures; this indicates a strong and frequent interaction with the serum proteins, at least at elevated temperature. In contrast, NPs grafted by the ALD-melt method remain in solution when the protein precipitates; this indicates a negligible interaction of the great majority of NPs.

Further evidence of the difference in stability in serum was the monitoring of the effective hydrodynamic size corresponding to the main number peak measured by DLS as function of time at 75°C (Fig. 5B). For ALD-melt-grafted NPs the predominant intensity peak shifted from 5nm hydrodynamic diameter (interpreted as being close to the average size of serum proteins) to ~15nm which corresponds well to the size measured for NPs alone. Thus, the result indicates a removal of protein from solution while the NPs stay suspended. In contrast, the one-step ligand exchange grafted NPs showed an early onset of aggregation and a reduction in hydrodynamic size of the main population. This could correspond to that the main residual in the supernatant after temperature-induced denaturation and precipitation consists of small and stable proteins in the serum, i.e. the NPs were efficiently precipitated while a fraction of protein remained. These observations support the interpretation of the visual inspection: a majority of NPs precipitate with the denatured serum protein for particles that do not reach high grafting densities, while densely grafted ALD-melt particles remain suspended. Thus, serum proteins are able to interact with and bind directly to the core of iron oxide NPs that are not densely grafted, while densely grafted NPs are efficiently shielded. The difference between relevant density regimes was found to be >0.5 chains/nm² of PEG(5kDa).

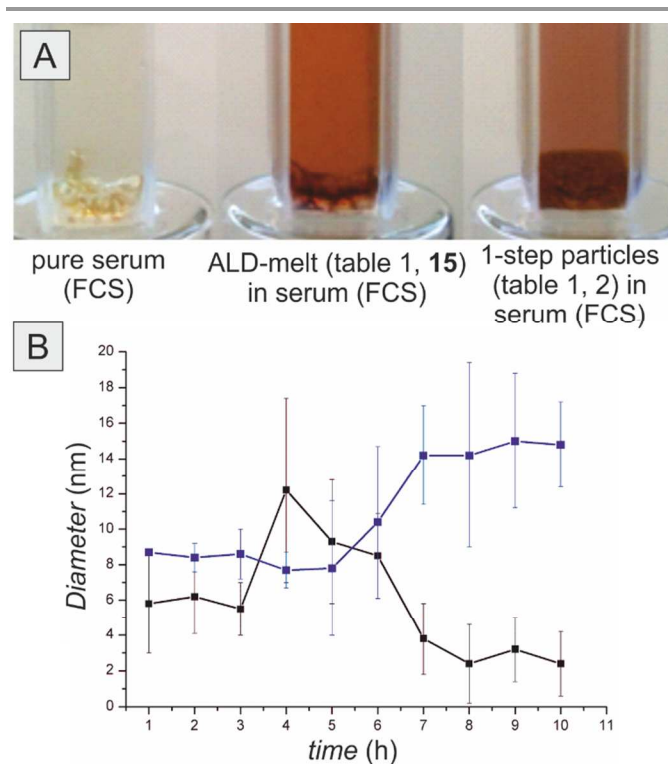


Figure 5. A): Pictures of different particles (ALD-melt particles, Table 1, 15 and one-step grafting-to particles, Table 1, 2) dissolved in fetal calf serum (FCS) and heated to 75°C for 10 hours. **B):** Effective hydrodynamic diameter measured as function of time by DLS on the serum solutions. The hydrodynamic diameter corresponding to the main number peak is shown. It shows a removal of the proteins from the ALD-melt sample (blue curve) and a removal of particles from the one-step grafting-to sample (black curve).

Concluding remarks

In summary, we have introduced grafting in a polymer melt to sterically stabilize monodisperse iron oxide NPs. Grafting of dense shells on such NPs requires replacement of the strongly physisorbed oleic acid remaining on the particle surface after synthesis; this has hitherto not been achieved and prevented biomedical application. The dispersant density and colloidal properties obtained by ALD-PEG grafted in a melt to NDA-primed iron oxide NP cores significantly surpass those of previously described methods in a direct comparison. Furthermore, the new method yields grafting densities that surpass any previously published system. In fact, the obtained dispersant densities approach the maximum defined by the density of nitrodopamine grafting sites on the primed iron oxide cores. Such high grafting densities should give rise to a brush density profile on the NPs that is unique,^{26, 27} and which is under further experimental investigation. A very high polymer density, close to the melt polymer density, would be expected close to the core surface; this would lead to a different type of brush density profile compared to previously achieved dispersant densities. The possibly different and denser brush profile might explain the observed unique properties in terms of rehydration and colloidal stability, e.g. direct dispersion with minimum addition of water and withstanding heat-induced

precipitation even in the presence of serum. Yields of ~30% could be achieved for two different core sizes, with further increased yield expected by improved NP dispersion in the polymer melt as well as more efficient reaction conditions, e.g. further improved removal of water produced during the reaction.

We emphasize that the principle of our method can be extended to other core-shell NP systems that require densely grafted flexible polymers; it is not limited to grafting of PEG nor to grafting to iron oxide cores. Using other suitably strongly binding anchor groups to present the reactive amine, we expect to extend the method to other types of NP cores. All kinds of polymers can in principle be grafted if their melt states are accessible without thermal decomposition or combustion taking place.

Acknowledgements

The research leading to these results received funding from the European Research Council under the European Union's Seventh Framework Programme (FP/2007-2013) / ERC Grant Agreement n. 310034. We thank Prof. Dieter Baurecht for access to FTIR. We acknowledge the VIBT Extremophile Center for access to TGA.

Notes and references

^a Institute for Biologically Inspired Materials, Department of Nanobiotechnology, University of Natural Resources and Life Sciences Vienna; Muthgasse 11-II, A-1190 Vienna, Austria

Electronic Supplementary Information (ESI) available: The supporting material contains details on additional synthetic protocols and characterization. This material is available free of charge via the Internet at

See DOI: 10.1039/c000000x/

1. M. Lewin, N. Carlesso, C.-H. Tung, X.-W. Tang, D. Cory, D. T. Scadden and R. Weissleder, *Nat. Biotechnol.*, 2000, **18**, 410-414.
2. M. J. Pittet, F. K. Swirski, F. Reynolds, L. Josephson and R. Weissleder, *Nat. Protocols*, 2006, **1**, 73-79.
3. A. Halbreich, J. Roger, J. N. Pons, D. Geldwerth, M. F. Da Silva, M. Roudier and J. C. Bacri, *Biochimie*, 1998, **80**, 379-390.
4. Q. A. Pankhurst, N. T. K. Thanh, S. K. Jones and J. Dobson, *J. Phys. D: Appl. Phys.*, 2009, **42**, 224001.
5. M. Namdeo, S. Saxena, R. Tankhiwale, M. Bajpai, Y. M. Mohan and S. K. Bajpai, *J. Nanosci. Nanotechnol.*, 2008, **8**, 3247-3271.
6. R. Weissleder, P. F. Hahn, D. D. Stark, E. Rummeny, S. Saini, J. Wittenberg and J. T. Ferrucci, *Am. J. Roentgenol.*, 1987, **149**, 723-726.
7. R. Weissleder, G. Elizondo, J. Wittenberg, C. A. Rabito, H. H. Bengel and L. Josephson, *Radiology*, 1990, **175**, 489-493.
8. J. R. McCarthy and R. Weissleder, *Adv. Drug Deliv. Rev.*, 2008, **60**, 1241-1251.
9. R. A. Sperling and W. J. Parak, *Philos. Trans. R. Soc., A*, 2010, **368**, 1333-1383.

10. E. Amstad, T. Gillich, I. Bilecka, M. Textor and E. Reimhult, *Nano Lett.*, 2009, **9**, 4042-4048.
11. J. Park, J. Joo, S. G. Kwon, Y. Jang and T. Hyeon, *Angew. Chem., Int. Ed.*, 2007, **46**, 4630-4660.
12. E. Amstad, M. Textor and E. Reimhult, *Nanoscale*, 2011, **3**, 2819-2843.
13. S.-J. Park, S. Kim, S. Lee, Z. G. Khim, K. Char and T. Hyeon, *J. Am. Chem. Soc.*, 2000, **122**, 8581-8582.
14. A. H. Lu, E. L. Salabas and F. Schueth, *Angew. Chem., Int. Ed.*, 2007, **46**, 1222-1244.
15. Y.-w. Jun, J.-H. Lee and J. Cheon, *Angew. Chem., Int. Ed.*, 2008, **47**, 5122-5135.
16. J. L. Dalsin, L. Lin, S. Tosatti, J. Vörös, M. Textor and P. B. Messersmith, *Langmuir*, 2004, **21**, 640-646.
17. E. Amstad, S. Zurcher, A. Mashaghi, J. Y. Wong, M. Textor and E. Reimhult, *Small*, 2009, **5**, 1334-1342.
18. T. Hyeon, S. S. Lee, J. Park, Y. Chung and H. B. Na, *J. Am. Chem. Soc.*, 2001, **123**, 12798-12801.
19. T. Gillich, C. Acikgöz, L. Isa, A. D. Schlüter, N. D. Spencer and M. Textor, *ACS Nano*, 2013, **7**, 316-329.
20. E. Amstad, A. U. Gehring, H. Fischer, V. V. Nagaiyanallur, G. Hahner, M. Textor and E. Reimhult, *J. Phys. Chem. C*, 2011, **115**, 683-691.
21. J. Park, K. An, Y. Hwang, J.-G. Park, H.-J. Noh, J.-Y. Kim, J.-H. Park, N.-M. Hwang and T. Hyeon, *Nature Materials*, 2004, **3**, 891-895.
22. J. Park, E. Lee, N.-M. Hwang, M. Kang, C. Kim Sung, Y. Hwang, J.-G. Park, H.-J. Noh, J.-Y. Kim, J.-H. Park and T. Hyeon, *Angew. Chem., Int. Ed.*, 2005, **44**, 2873-2877.
23. S. G. Kwon, Y. Piao, J. Park, S. Angappane, Y. Jo, N.-M. Hwang, J.-G. Park and T. Hyeon, *J. Am. Chem. Soc.*, 2007, **129**, 12571-12584.
24. S. Mondini, A. M. Ferretti, A. Puglisi and A. Ponti, *Nanoscale*, 2012, **4**, 5356-5372.
25. E. Amstad, J. Kohlbrecher, E. Müller, T. Schweizer, M. Textor and E. Reimhult, *Nano Lett.*, 2011, **11**, 1664-1670.
26. F. Lo Verso, S. A. Egorov, A. Milchev and K. Binder, *J. Chem. Phys.*, 2010, **133**.
27. G. G. Vogiatzis and D. N. Theodorou, *Macromolecules (Washington, DC, U. S.)*, 2013, **46**, 4670-4683.